Control of Metal Nanoparticles Aggregation and Dispersion by PNA and PNA−DNA Complexes, and Its Application for Colorimetric DNA Detection

Xiaodi Su* and Roejarek Kanjanawarut

Institute of Materials Research and Engineering, A*STAR (Agency for Science, Technology and Research), 3 Research Link, Singapore 117602

ABSTRACT We have demonstrated that mixed-base PNA oligomers are effective coagulants of citrate ion-coated gold and silver nanoparticles (AuNPs and AgNPs), and PNA-induced particle aggregation can be disrupted by hybridization of PNA with a specific DNA. Using particles' aggregation/dispersion as a measure, we have investigated how PNA and PNA−DNA complexes bind to AuNPs and AgNPs and modulate particles' stability differently relative to their DNA counterparts. We have made the following original discoveries: (1) mix-base PNA oligomers can induce immediate particle aggregation in a concentration- and chain-length-dependent manner; (2) PNA oligomers have a higher affinity to AuNPs and AgNPs than its ssDNA counterpart; (3) PNA−DNA complexes, although having a stable double helix structure similar to dsDNA, can effectively protect the particles from salt induced aggregation, and the protection effect of different nucleic acids are in the order of PNA−DNA complex > ssDNA > dsDNA; (4) all the characteristics are identical for AuNPs and AgNPs; and (5) AgNPs is more sensitive in response to destabilization effect and is proven a more sensitive platform for colorimetric assays. The control of particle aggregation and dispersion by PNA and PNA−DNA complexes has been used to detect a specific DNA sequence with single-base-mismatch resolution. ζ potential measurements have been conducted to reveal how distinct backbone properties of PNA and PNA−DNA complexes relative to their DNA counterparts contribute to the distinct binding characteristics.

KEYWORDS: gold nanoparticles · silver nanoparticles · colorimetric assay · peptide nucleic acids · DNA hybridization · single-base-mismatch discrimination

The interaction of DNA with citrate ion-protected gold nanoparticles (AuNPs) has been a subject of extensive studies due to its remarkable utility in nanoassembly and bioassays.[1−4] Using spectroscopy techniques (*e.g.*, Raman spectroscopy, SERS, FTIR), quasielastic light scatter, isothermal titration calorimetry, ζ potential measurement, as well as AuNPs' aggregation as a measure, interactions between AuNPs and nucleobases,[5,6] nucleosides,[7,8] mononucleotides,[9] and oligonucleotides[10−13] have been characterized in great detail, including sequence-dependent binding affinity,[5,6,8,9] the coordinating process of nucleosides on gold,[7] chain-length-dependent binding kinetics of ssDNA,[11] the distinct binding property of ssDNA and dsDNA,[10−13] and DNA structure-dependent displacement of citrate ions.[14] These characteristics are not only of theoretical significance but also practically useful to guide bioassay design, particularly the particle aggregation-based colorimetric assays.[2−4] The characteristics that ssDNA is able to absorb on AuNPs whereas dsDNA has limited affinity to AuNPs, for example, have been used to design "noncrosslinking" aggregation-based DNA hybridization assays,[10−13] ligand−aptamer binding assays,[15,16] and DNAzyme cleavage assay.[17] In these assays, coating of negatively charged ssDNA to AuNPs causes the particles to gain negative charges and resistance to salt-induced aggregation, whereas dsDNA or structured DNA are unable to protect AuNPs against salt-induced aggregation.

Peptide nucleic acids (PNA) are DNA analogues in which the entire sugar−phosphate backbone is replaced by a charge neutral polyamide backbone. The superior hybridization properties of PNA arising from its distinct backbone properties (charge neutrality and high rigidity) have enabled PNA to be an important supplement of DNA in many applications. In contrast to the large body of characteristics available for DNA−AuNPs interactions, however, PNA−AuNPs interactions have been less well studied, except one for PNA base monomers.[5] The involvement of PNA in AuNPs-based nanoassembly and bioassays is also much fewer, with merely, to the best of our knowledge, two studies reporting

*Address Correspondence to xd-su@imre.a-star.edu.sg.

Received for review June 2, 2009 and accepted August 17, 2009.

Published online August 26, 2009. 10.1021/nn9005768 CCC: $40.75

preparation of stable PNA−AuNPs conjugates for nanoassembly and for DNA detection applications.[18,19]

We have recently observed that mixed-base PNA oligomers (no additional modification at the C- and N-terminals) can induce immediate aggregation of gold and silver nanoparticles (AuNPs and AgNPs), and the aggregation can be greatly disrupted by PNA hybridization to a specific DNA.[20] The control of particle aggregation and dispersion by PNA and its DNA complex hint that these nucleic acids can bind to citrate ion coated metal nanoparticles and modulate the particles' surface property. Inspired by the large extent of binding characteristics available for DNA, we have conducted a systematic study of how PNA and PNA−DNA complex interact with AuNPs, as well as AgNPs, in a concentration-, sequence-, and chain-length-dependent manner, using particles' aggregation/dispersion as a measure. A number of original observations have been made on how PNA and PNA−DNA complex modulate nanoparticles' stability differently relative to their DNA counterparts (ssDNA and dsDNA). ζ potential measurement has been conducted to measure surface charge density and to assist the discussion of the distinct electrostatic, steric, and electrosteric effects of PNA and PNA−DNA complex, arising from their distinct backbone properties. AuNPs and AgNPs of 13 and 16 nm in diameter, respectively, were used in this study. These are the most commonly used particle size in nucleic acid adsorption studies and in bioassays. Thus, the results obtained here would be representative of common interests.

Motivated by the growing efforts to develop robust colorimetric assays using unmodified metal nanoparticles and innovative aggregation principle,[10−17,20−24] we have applied the PNA/PNA−DNA complex controlled nanoparticle aggregation/dispersion to detect a specific DNA sequence with single-base-mismatch resolution. Unlike the assays using the distinct electrostatic properties of ssDNA and dsDNA,[10−13] this current assay uses PNA as a "coagulant" to alter the intrinsic stability of AuNPs (and AgNPs), and no salt is needed to induce particle aggregation. This "coagulation" mechanism has been largely used for constructing enzymatic activity assays[21−25] but yet applied for designing DNA hybridization assay except for our group.

RESULTS AND DISCUSSION

PNA-Induced AuNPs Aggregation. Inspired by the extensive understanding on the binding characteristics of ssDNA with AuNPs,[10−13,17] we conducted a detailed study of PNA-induced AuNPs aggregation with the involvement of four mixed-base PNA oligomers of different chain length (10-, 13-, 20-, and 22-mer) and base composition, aiming to extract PNA−AuNPs binding characteristics in terms of concentration, sequence, and chain length dependence.

Parts A and B of Figure 1 are representative UV−vis adsorption spectra of AuNPs mixed with the 13-mer and 22-mer PNA (PNA_{13} and PNA_{22}) at different concentrations. The shift of surface plasmon peak from 520 nm to longer wavelengths evidences the particle aggregation. The degree of aggregation is found to be determined by PNA concentration. The plots of aggregation degree (measured as ratio of absorbance at 600 and 520 nm, A600/A520) *versus* PNA concentration for all four PNAs (Figure 1C) show that the shorter PNA_{10} and PNA_{13} aggregate the particles more effectively than the longer ones (PNA_{20} and PNA_{22}) at any given concentration. This implies that the shorter PNAs cover the AuNPs more effectively than the longer ones. This characteristic resembles what is known for ssDNA,[11] which has been rationalized as the shorter ones having a less coiled structure that ensures the nucleobases to be exposed more easily. As for the sequence effect, the similar aggregation efficiency of PNA of similar length but different base composition (10- and 13-mer; 20- and 22-mer) shows that the multivalent interaction between

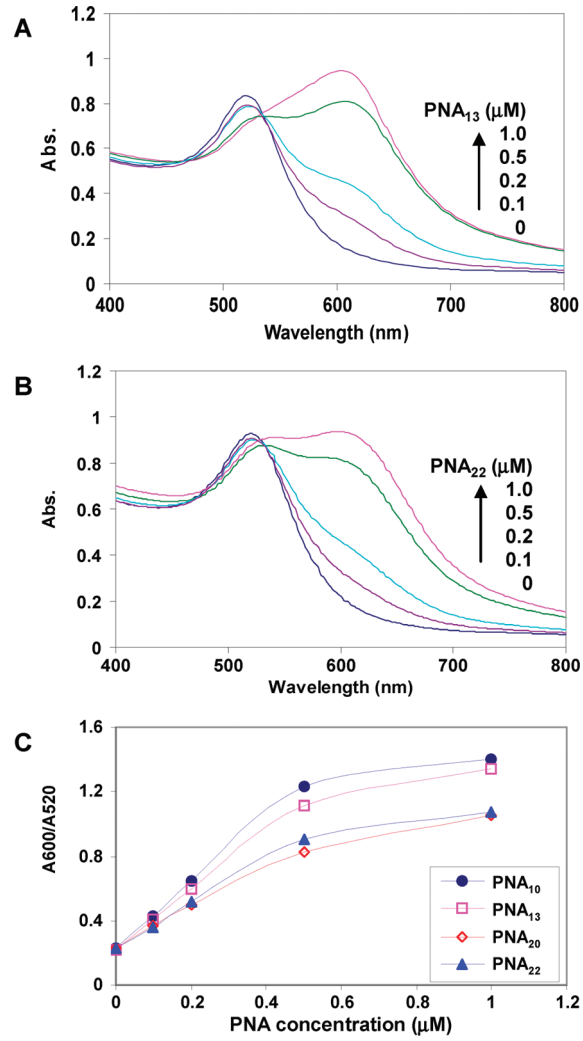

Figure 1. PNA-induced AuNPs aggregation. UV−vis adsorption spectra of AuNPs (13 nm in diameter) exposed to (A) 13-mer PNA_{13} and (B) 22-mer PNA_{22} at different concentrations. (C) Plots of aggregation degree (measured as A600/A520) *versus* PNA concentration for the 10-, 13-, 20-, and 22-mer PNAs.

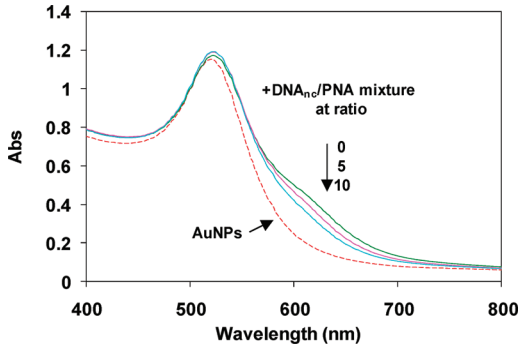

Figure 2. PNA has a higher affinity to AuNPs than its ssDNA counterpart. UV−vis adsorption spectra of bare AuNPs and AuNPs after 10 min incubation with a mixture of PNA_{22} (200 nM) and ssDNA of same sequence (termed as $noncDNA_{nc}$) at DNA/PNA ratio of 0, 5, and 10.

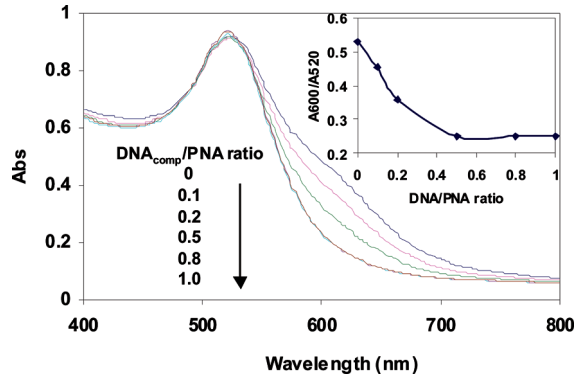

Figure 3. PNA−DNA hybridization disrupts particle aggregation. UV−vis adsorption spectra of AuNPs solutions after 10 min incubation with PNA_{22} (200 nM) annealed with its complementary DNA_{comp} at 0, 20, 40, 100, and 160 nM. The inset is the plot of aggregation degree (measured as A600/A520) *versus* DNA/PNA ratio.

mixed-base PNA and AuNPs is not sensitive to the base sequence.

To better understand the mechanism of PNA-induced AuNPs aggregation, we measured the surface charge of AuNPs before and after PNA coating (PNA_{13} was used as an example). We found that PNA_{13}-coated AuNPs has a similar charge density (ζ potential −20.11 ± 3.6 mV) as compared to the uncoated AuNPs (ζ potential −21.04 ± 2.6 mV). This suggests that the PNA coating only shields the citrate ions (no displacement occurs). This concurs with Li and Rothberg's Raman spectroscopy result for single-stranded oligonucleotides (ssDNA), showing that coating of ssDNA on AuNPs did not displace citrate ions.[10] However, the inability of charge neutral PNA oligomers to displace citrate ions from gold surface appears to conflict with previous studies for other charge neutral substances, *e.g.*, adenosine,[21] nucleobases,[5,6] and nucleosides.[8] Coating of these small molecules has been proven to be able to displace weakly bound citrate ions from AuNPs. It might be the steric hindrance arising from the polymer structure of the PNA oligomers makes the binding not strong enough to displace the citrate ions. Using DNA as a example, Zhao *et al.* did report that ssDNA oligonucleotides bind less effectively to AuNPs than mononucleosides due to larger molecular size.[9]

PNA Binds More Strongly to AuNPs than Its ssDNA Counterpart. ssDNA is known to be able to adsorb on AuNPs and to stabilize colloidal suspensions in high salt concentration.[10−13,17] However, in the presence of PNA, we found ssDNA's stabilization effect is abolished. Figure 2 shows the stability of AuNPs solutions exposed to mixtures of PNA_{22} (200 nM) and ssDNA of the same sequence (no hybridization occurs) at a ssDNA/PNA_{13} ratio of 0, 5, and 10. Figure S1 (Supporting Information) shows the result with the 20-mer PNA_{20} at a higher concentration (1 μM) and same range of ssDNA/PNA ratio. Both Figure 2 and Figure S1 (Supporting Information) show that PNA-induced particle aggregation remains largely detectable when ssDNA is in great excess. When NaCl is added, further aggregation was observed regardless the presence of ssDNA (ssDNA alone at the above tested concentrations is sufficient to protect AuNPs to against salt induced aggregation; see Figure 4 and related discussion).

The abolishment of ssDNA's protection effect when PNA is present gives strong evidence that PNA binds dominantly to AuNPs relative to ssDNA. We believe that the distinct backbone properties of PNA (neutrality, high rigidity, and peptide composition) are attributable to its higher affinity to gold. The neutrality ensures no charge repulsion between PNA and citrate-coated AuNPs as severely encountered by negatively charged ssDNA. The high backbone rigidity renders the nucleobases to be exposed more effectively than those in coiled ssDNA. The peptide composition introduces secondary interaction with gold.[5]

Stabilization Effect of PNA−DNA Complex. Apart from the fact that noncomplementary DNA (denoted as DNA_{nc}) has little interference to PNA-induced AuNPs aggregation, further experiments with complementary DNA_{comp} show that the presence of a small amount of DNA_{comp} can disrupt the particle aggregation significantly. Figure 3 shows the discriminative stability of AuNPs solutions mixed with PNA_{22} (200 nM) and PNA_{22} annealed with its fully complementary target DNA_{comp} at DNA/PNA ratio of 0.1 to 1. The PNA-induced particle aggregation is depleted gradually with the increase of DNA_{comp} concentration until being abolished at DNA/PNA ratio of 0.5. Apparently, the depletion of particle aggregation in the presence of DNA_{comp} is due to the reduction of free PNA upon formation of the PNA−DNA complex. The observation that particle aggregation is abolished when half of the PNA (at DNA/PNA ratio of 0.5) being consumed is evidence that the as-formed PNA−DNA complex prevents the remaining PNA (100 nM in this case) from aggregating the particles (PNA_{22} at 100 nM is sufficient to induce detectable aggregation in the absence of other species, Figure 1B). This is a primary hint that PNA−DNA complex has certain affinity

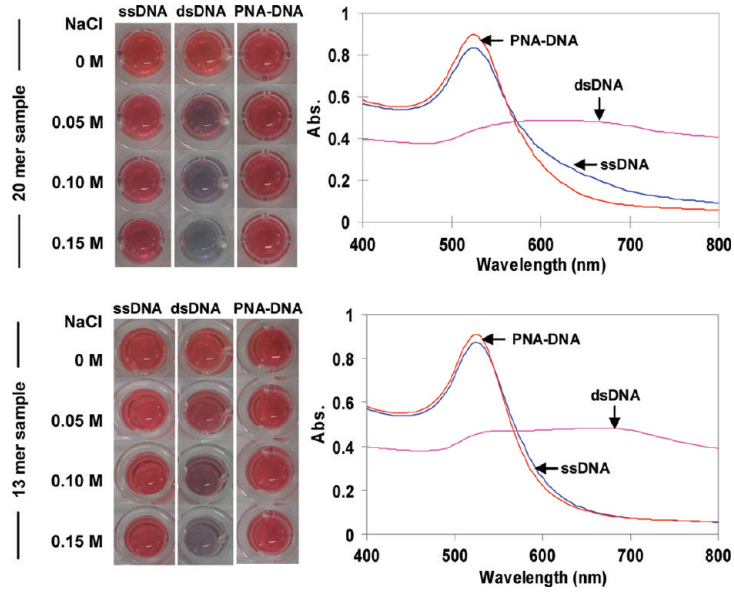

Figure 4. Stabilization effects of different nucleic acids to AuNPs. Photographs of AuNPs solutions taken after 10 min incubation with ssDNA, dsDNA, and PNA−DNA complex (20-mer and 13-mer samples), without and with addition of NaCl (0.05, 0.1, and 0.15 M) at the end of incubation. The respective UV−vis adsorption spectra are for solutions with 0.15 M NaCl. The final concentration of all nucleic acids samples is 1 μM.

to AuNPs. The binding of the PNA−DNA complex provides sufficient protection to AuNPs to overcome PNA's destabilization effects.

To further understand the binding property of PNA−DNA complex to AuNPs and to compare its protection of AuNPs relative to ssDNA and dsDNA, PNA_{13} and PNA_{20} and their corresponding complementary DNA of equal amount were annealed to form PNA−DNA complexes. The incubation solutions were then mixed with AuNPs. The stability of the colloidal solutions before and after addition of salt was recorded (Figure 4). Before addition of NaCl, the solutions with ssDNA, dsDNA, and PNA−DNA complex are all stable as indicated by their red color and sharp SP peaks around 520 nm. Slight peak wavelength and peak intensity difference are a primary indication of the adsorption of different nucleic acid samples to gold that leads to the local change of the dielectric permittivity (spectra before adding salt not shown). After NaCl is added, the dsDNA-containing solutions gradually aggregated as expected. With the increase of NaCl concentration, the color changes from red to purple and blue. However, the other solutions containing either PNA−DNA complex or ssDNA remain in red color, even at the highest NaCl concentration tested. From the similar color code of these two types of solutions, one can not deduct a stability difference; whereas their UV−vis adsorption spectra (at 0.15 M NaCl) reveal a noticeable difference in particles' stability. For both the 13- and 20-mer samples, the ssDNA-containing solutions are less stable than the PNA−DNA containing solutions, showing a noticeable red-shift of the spectrum.

It is well-known that duplex DNA (dsDNA) has little affinity to negatively charged AuNPs due to its stable DNA−DNA double-helix geometry that always isolates the nucleobases and presents the negatively charged phosphate backbone. As a result, dsDNA cannot protect AuNPs from salt-induced aggregation, as compared to ssDNA.[10−13,17] Our discovery that despite the presence of double-helix geometry PNA−DNA duplexes can effectively protect AuNPs against salt-induced aggregation, better than dsDNA and even ssDNA, is an interesting phenomenon. We have rationalized this phenomenon from both the electrostatic and steric stands. First of all, a PNA−DNA duplex carries only half of the negative charges relative to its dsDNA counterpart. Under the low ionic strength conditions used in this experiment (<3 mM NaCl, see the Methods), the effective charge of PNA−DNA complex would be noticeably lower than that of dsDNA. This would enable the PNA−DNA complex to adsorb more effectively than dsDNA onto citrate ion-coated AuNPs, due to depleted charge repulsion. Second, the nitrogen-/oxygen-containing peptide backbone of the PNA strand can interact with gold,[5] leading to a higher affinity than dsDNA. In a comparison between PNA−DNA complex and ssDNA, both having similar charge density but entirely different structure properties (insulated or exposed bases), we are not able to speculate which one binds more effectively to gold with a higher affinity without characterizations using other techniques. But the stronger protection of PNA−DNA than ssDNA could be largely or at least partially attributable to the larger molecular size and the structure rigidity of PNA−DNA complex that introduces more steric protection than ssDNA. This interpretation is indirectly supported by the fact that the stability difference between PNA−DNA complex- and ssDNA-protected AuNPs is larger for the 20-mer samples than the 13-mer samples (more obvious UV−vis spectra difference in Figure 4A than in 4B). It would be expected that the steric effect of the larger PNA−DNA duplexes is more obvious than the smaller ones.

The hypothesis that steric effect, rather than charge effect, is attributable for the better stability of PNA−DNA complex-protected AuNPs than ssDNA-protected ones has been further supported by ζ potential measurement (using the 13-mer sample as example). In 0.15 M NaCl, the ζ potentials of AuNPs coated with PNA−DNA, ssDNA, and dsDNA are -31.2 ± 8.2, -30.7 ± 6.7, and -10.4 ± 7.3 mV, respectively. The charge density of the PNA−DNA complex- and ssDNA-protected AuNPs are similar, meaning that electrostatic repulsion is similar. Thus, the observed differential stability should be a result of differential steric effect. For the dsDNA-protected particles, the high ζ potential

value, indicating of reduced surface charge and reduced electrostatic repulsion, explains why aggregation occurs easily.

By far, we have completed a whole picture of nucleic acids−AuNPs interaction and the stabilization effects of different nucleic acid samples, as sketched in Figure 5. In particular, with the 13 nm AuNPs, whose diameter is comparable with the molecular contour length of the 10−22-mer nucleic acids samples, we have demonstrated that (1) mixed-base PNA oligomers can induce immediate particle aggregation, (2) PNA oligomer have a higher affinity to NPs than its ssDNA counterpart, (3) PNA−DNA complex, although having a stable double helix structure similar to dsDNA, can effectively protect NPs from salt induced aggregation, and (4) the ability of different nucleic acids to protect AuNPs against salt-induced aggregation is in the order PNA−DNA complex > ssDNA > dsDNA. An in-depth concern about how NPs with much larger or smaller size relative to nucleic acids' molecular contour length modulate the adsorption behavior will be subject to further studies.

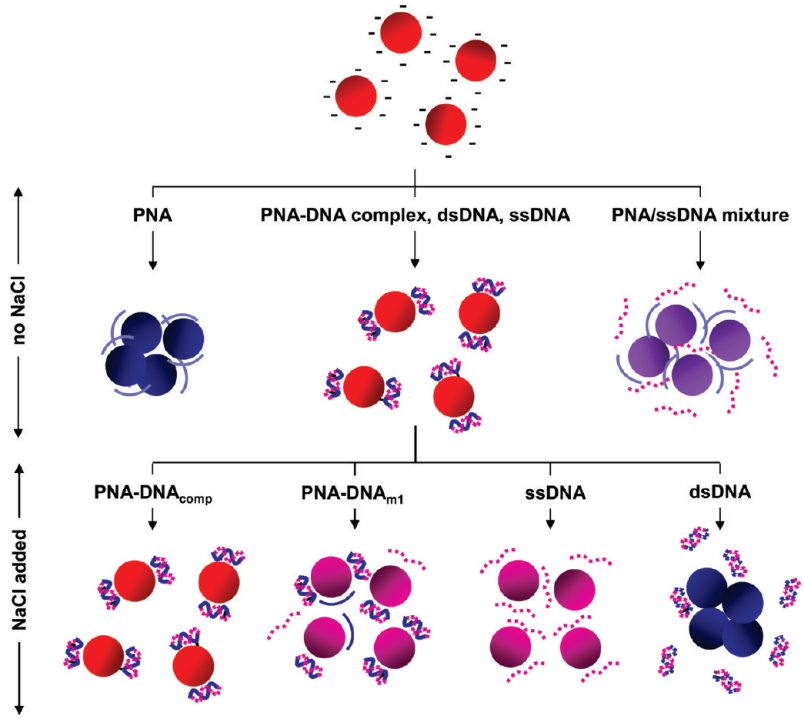

Figure 5. Schematic illustration of how different nucleic acids (PNA, PNA−DNA complexes, ssDNA, dsDNA, and PNA/DNA mixture) affect AuNPs' intrinsic stability and AuNPs' stability against salt.

Nucleic Acids' Binding Characteristics to AgNPs. AgNPs have a higher extinction coefficient relative to AuNPs of the same size. It is therefore believed that AgNPs would have a higher sensitivity for use in colorimetric assays.[22,26,27] We have conducted experiments with citrate ion protected AgNPs to extend the understanding of nucleic acid−AgNPs interactions and to address the sensitivity merit of this material for this particular application.

Figure 6 shows the stability of AgNPs solutions incubated with ssDNA, dsDNA, PNA−DNA complex, and PNA (13-mer samples). From the color photographs and the UV−vis adsorption spectra, we have made the following observations: (1) mixed-base PNA can induce immediate AgNPs aggregation, characterized as color change from yellow to brown and the drop of absorbance at the original SP peak (~400 nm) and the appearance of SP peak at longer wavelength; (2) PNA−DNA hybridization disrupts the PNA-induced aggregation; and (3) PNA−DNA complex, ssDNA, and dsDNA do not affect AgNPs' intrinsic stability, but when NaCl is added, dsDNA-containing AgNPs aggregates immediately at the lowest NaCl concentration tested, ssDNA-containing AgNPs aggregates slowly with the increase of salt concentration, and the PNA−DNA complex-containing AgNPs remains stable up to the highest salt concentration tested. With these observations, we confirm that nucleic acids' binding characteristics and their stabilization effects are identical for AuNPs and AgNPs. The well-known characteristic that ssDNA, but not dsDNA, can protect AuNPs against salt-induced aggregation[9−13] is, for the first time, proven true for AgNPs. With this experiment we also found AgNPs is more sensitive in response to small difference in stabilization effect. Our original discovery that PNA−DNA complex can better protect nanoparticles against salt-induced aggregation than ssDNA is further confirmed with AgNPs, *via* both the color change and UV−vis spectrum shift, whereas with AuNPs, only a slight spectrum shift is accountable for this characteristic (Figure 4).

Detection of Preannealed PNA−DNA Complex with Single-Base-Mismatch Sensitivity Using AuNPs and AgNPs. We have shown previously that successful hybridization of PNA with its complementary DNA$_{comp}$ can abolish PNA-induced particle aggregation. In the case where target DNA contains a single-base-mismatch (DNA$_{m1}$), the less effective hybridization (or higher tendency of dehybridization) would cause some PNA to remain free in solution. We thus anticipate that the unhybridized PNA would aggregate the particles, detectable by typical spectrum shifts. Figure 7 shows the experimental validation using the 13-mer sample. In the absence of NaCl, the UV−vis curves of the NPs solutions containing PNA annealed with DNA$_{m1}$ carry a small but noticeable signature of particle aggregation, *i.e.*, an increase of A600 of 3.5% for AuNPs and an increase of A600/A400 of 10.8% for AgNPs, relative to those with fully complementary DNA$_{comp}$. These spectra shifts are significant compared to the variation of A600 measurement for AuNPs (1.03%) and A600/A400 measurement for AgNPs (0.97%) (Figures S2 and S3 and Table S1, Supporting Information). When NaCl is added to enhance the stringency, the discrimination between DNA$_{comp}$ and

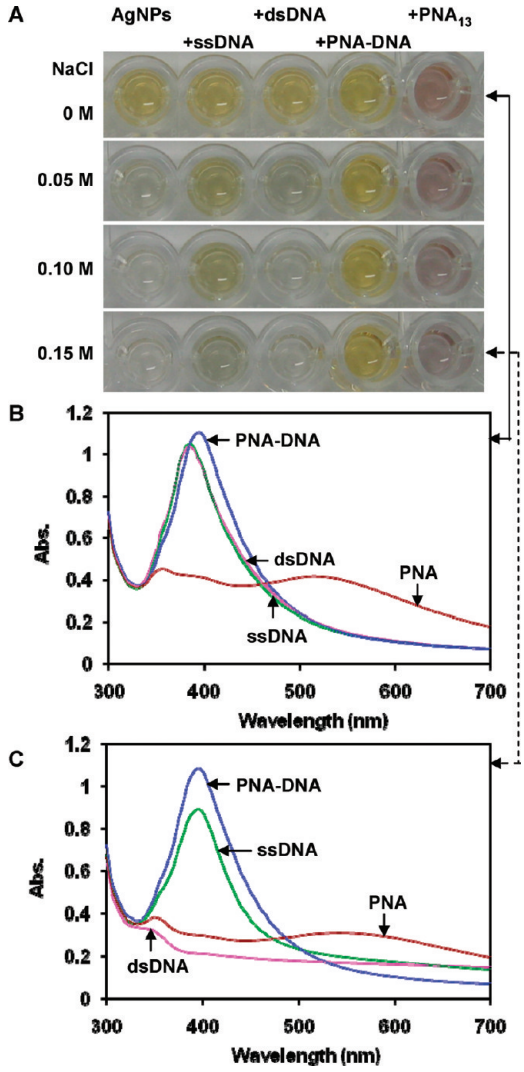

Figure 6. Stabilization effects of different nucleic acids to AgNPs. (A) Photographs of AgNPs solutions recorded after 10 min incubation with ssDNA, dsDNA, PNA−DNA complex, and PNA (13-mer samples), without and with addition of NaCl (final concentration 0.05, 0.1, and 0.15 M) at the end of incubation. (B) and (C) are corresponding UV−vis adsorption spectra before and after addition of NaCl (0.15 M), respectively. The final concentration of all nucleic acids is 1 μM.

DNA_{m1} is enlarged. For AuNPs, the ΔA600 value increases to 8.5%, 11.0%, 15.3%, and 21.1% at NaCl concentrations of 0.1, 0.2, 0.3, and 0.4 M, respectively; for AgNPs, the ΔA600/A400 increases to 23.9%, 108.7%, 291.6%, and 316.5% at the same NaCl concentration range. At a fixed salt condition, a larger degree of differentiation is observed for AgNPs, which proves again that AgNPs is more sensitive in response to small difference in stabilization effect and is a more sensitive colorimetric platform for single-mismatch detection.

Detection of PNA Hybridization with DNA in Preincubated DNA/AuNPs Mixtures. According to the characteristic that PNA has a stronger affinity to AuNPs than ssDNA, we have designed an alternative approach to detect a specific DNA through PNA−DNA hybridization in a DNA/AuNPs mixture but not through post addition of preannealed PNA−DNA complex. This approach is designed on the basis of our speculation that PNA is able to strip DNA from the AuNPs surface and further hybridize to the DNA if the sequences are complementary. Figure 8A shows the results with the 13-mer samples. Prior to PNA addition, AuNPs solutions mixed with different target DNA (DNA_{comp}, DNA_{m1}, and DNA_{nc}) are all in red, showing a good dispersion state. When PNA_{13} is added, gradual color changes are developed in the single-base-mismatch (DNA_{m1}) and noncomplementary (DNA_{nc}) wells, but not in the complementary DNA_{comp} well. This confirms our speculation that PNA can displace adsorbed DNA and induces particle aggregation when it is free from hybridization (in the case of DNA_{nc}) or hybridizes in a lower efficiency (the case with DNA_{m1}), whereas when the sequences are complementary, displacement of DNA is accompanied by an effective PNA−DNA hybridization. The resulting PNA−DNA complexes keep the AuNPs stable.

The same experiment was repeated with the PNA_{22} and its target DNA (DNA_{comp}, DNA_{m1}, and DNA_{nc}) (Figure 8B). Interestingly, we found that with time passes (up to 2 h), no obvious color changes are developed in any of the wells upon PNA_{22} addition, which means that PNA_{22} failed to displace (and hybridize with) the adsorbed ssDNA from AuNPs surface or the displacement is insignificant. This discrepancy relative to the PNA_{13} could be explained by our previous discovery that a longer PNA is less effective than a shorter one to coat on AuNPs. To further confirm our speculation that there might be a small degree of displacement of DNA by PNA_{22} (too small to induce particle aggregation), NaCl was added to screen the negative charges. Upon a proper selection of salt concentration (0.025 and 0.05 M), obvious color discrimination is observed between wells containing DNA_{comp}, DNA_{m1}, and DNA_{nc}, respectively. The color changes to dark red (for DNA_{m1}) and to purple/blue (for DNA_{nc}) are an indication of particle aggregation. The retained stability of AuNPs in the DNA_{comp} well with the exposure to NaCl must be originated from the formation of PNA−DNA complex which has a strong ability to protect AuNPs, as demonstrated using the preannealed PNA−DNA complex earlier.

The successful discrimination of single-base-mismatch using PNA- and PNA−DNA complex-controlled AuNPs/AgNPs aggregation/dispersion demonstrates the advantageous of the colorimetric assay relative to the solid−liquid phase hybridization assay, *e.g.*, using surface plasmon resonance spectroscopy (SPR). With the SPR measurement of DNA hybridization to immobilized PNA probes, no discrimination is detectable between DNA_{comp} and DNA_{m1} for the 13-mer sample (Figure S4, Supporting Information) and for the 22-mer sample,[28] unless stringent hybridization conditions are used.

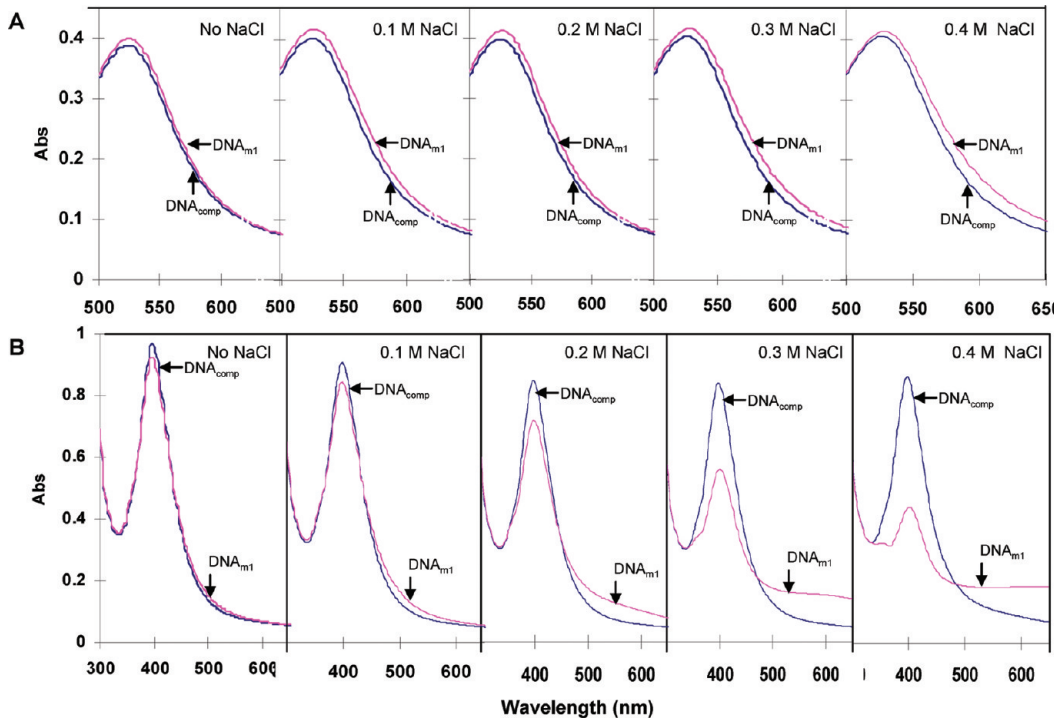

Figure 7. Single-base-mismatch discrimination in preannealed PNA−DNA complexes. UV−vis adsorption spectra of (A) AuNPs and (B) AgNPs after 10 min incubation with PNA_{13} preannealed with complementary (DNA_{comp}, blue curves) and single-base-mismatch (DNA_{m1}, pink curves) targets, without and with addition of NaCl (0−0.4 M) at the end of incubation. Final nucleic acid concentration is 1 μM.

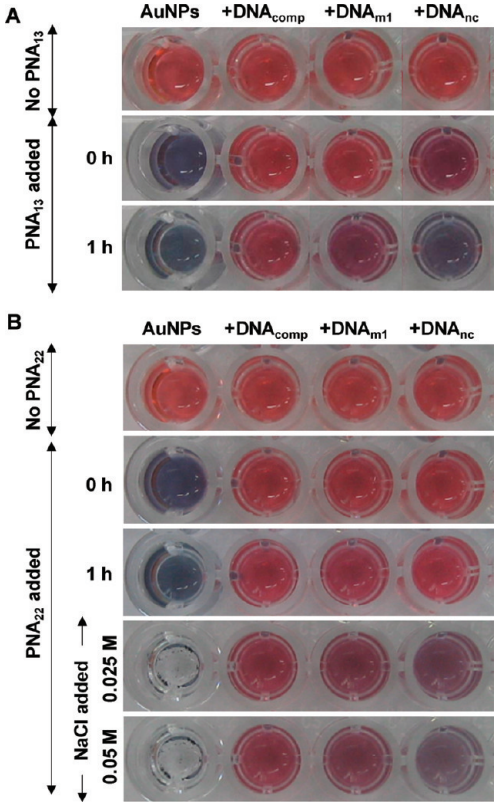

Figure 8. Colorimetric detection of PNA hybridization with DNA in DNA/AuNPs mixtures. Color photographs of AuNPs and AuNPs mixed with DNA_{comp}, DNA_{m1}, and DNA_{nc} (final concentration 1 μM) of (A) 13-mer and (B) 22-mer samples, before and after addition of respective PNA (final concentration 1 μM). NaCl is further added into the 22-mer sample wells.

CONCLUSIONS

Using metal nanoparticles' aggregation/dispersion as a measure, we have studied how mixed-base PNA oligomers and their PNA−DNA complexes interact with AuNPs and AgNPs. We have made a number of original observations to show that PNA and PNA−DNA complex have distinct binding behaviors relative to their DNA counterparts originated from their distinct backbone properties. Through a parallel study with AuNPs and AgNPs, we have shown that nucleic acids' binding characteristics are identical to AuNPs and AgNPs; and AgNPs is more sensitive in response to changes in stabilization effects, making it a more sensitive platform for colorimetric assays. Making use of the controlled particle aggregation/dispersion by PNA/PNA−DNA complex, DNA detection with single-base-mismatch sensitivity has been achieved.

TABLE 1. PNA and DNA Sequences

length	name	sequences
10-mer	PNA_{10}	N′-ATCTTCTAGT-C′
13-mer	PNA_{13}	N′-TTCCCCTTCCCAA-C′
	DNA_{comp}	5′-TTGGGAAGGGGAA-3′
	DNA_{m1}	5′-TTGGGAGGGGGAA-3′
20-mer	PNA_{20}	N′- TTGCACTGTACTCCTCTTGA-C′
	DNA_{comp}	5′-TCAAGAGGAGTACAGTGCAA-3′
22-mer	PNA_{22}	N′-AACCACACAACCTACTACCTCA-C′
	DNA_{comp}	5′-TGAGGTAGTAGGTTGTGTGGTT-3′
	DNA_{nc}	5-CAAAACAAAGATCTACATGGAT-3′
	DNA_{m1}	5′-TGAGGTAGTAAGTTGTGTGGTT-3′

METHODS

Reagents. $HAuCl_4 \cdot 3H_2O$ (99.99%) and $AgNO_3$ (99.9%) were obtained from Alfa Aesar (MA). Trisodium citrate dihydrate (99.9%) was obtained from Aldrich and $NaBH_4$ from Fluka. Concentrated HCl and HNO_3 were all analytical grade and used without further purification. Mixed-base PNA oligomers of 10-, 13-, 20-, and 22-mer (denoted as PNA_{10}, PNA_{13}, PNA_{20}, and PNA_{22}) with no modification at C- and N-terminals, were synthesized by the Eurogentec S.A. Leige (Belgium). Target DNA of fully complementary (DNA_{comp}), noncomplementary (DNA_{nc}), and single-base-mismatch sequence (DNA_{m1}) were from Proligo-Sigma (for PNA and DNA sequences, see Table 1).

Colloidal Preparation. Citrate-stabilized AuNPs were prepared by thermal reduction of $HAuCl_4$ with sodium citrate.[29] Citrate-stabilized AgNPs were synthesized by the reduction of silver nitrate using sodium borohydride.[22] Spherical AuNPs of 13.2 $\pm$ 1.1 nm and AgNPs of 16.1 $\pm$ 0.6 nm were observed under TEM. The concentrations of the AuNPs and AgNPs were 7.3 and 0.39 nM, respectively, calculated according to Beer's law, using the extinction coefficient of 2.7×10^8 M^{-1} cm^{-1} for 13 nm AuNPs[30] and 9.4×10^9 M^{-1} cm^{-1} for 16 nm AgNPs.[31,32]

Characterization. Ninety-six-well microplates were used as reaction carrier. UV−vis absorption characterization was performed using a TECAN infinite M200 (Tecan Trading AG, Switzerland). The reproducibility of the UV−vis absorption spectrum measurement (at room temperature) was evaluated through multiple scans of a given AuNPs (and AgNPs) solution aliquot in different wells. The variation of the absorbance measurement at representative wavelengths is ~1% for AuNPs and within 2% for AgNPs (Figures S2 and S3 and Table S1, Supporting Information). ζ potential measurements were preformed on bare AuNPs and PNA-, PNA−DNA complex-, ssDNA-, and dsDNA-coated AuNPs in water or in 0.15 M NaCl, using a ZETA PLUS zeta potential analyzer (Brookhaven Instruments). A mixture of AuNPs (7.3 nM) and nucleic acid samples (1 μM) of 450 μL was diluted into 2 mL for the measurement.

Assay Procedure. To test the coagulating property of PNA, aliquots of stock PNA probes (100 μM) were added to 150 μL of AuNPs (or AgNPs) solution. After 10 min incubation at room temperature, the color of the solutions was recorded using a camera and the absorption spectra were recorded in a wavelength range of 400−800 nm for AuNPs and 300−800 nm for AgNPs. To measure the ability of PNA−DNA complex and dsDNA to protect AuNPs (or AgNPs) and to detect the sequence specific hybridization, the PNA (or DNA) probe and DNA target of equal amount (40 μM) were annealed in 20 mM phosphate buffer (pH 7.2, containing 100 mM NaCl, and 0.1 mM EDTA), prior to addition to nanoparticle solutions (150 μL) (final DNA concentration 1 μM). When necessary, NaCl (final concentration 0.1−0.4 M) was added to accelerate particle aggregation. To test PNA hybridization with DNA inside AuNPs solution, DNA was first mixed with AuNPs (final DNA concentration 1 μM, final buffer concentration is 1 mM PBS). After 10 min incubation, PNA (final concentration 1 μM) was added.

Supporting Information Available: AuNPs aggregation in the presence of PNA/ssDNA mixture, reproducibility of UV−vis adsorption spectrum measurement, and DNA hybridization with 13-mer PNA measured by SPR. This material is available free of charge *via* the Internet at http://pubs.acs.org.

REFERENCES AND NOTES

1. Daniel, M. C.; Astruc, D. Gold Nanoparticles: Assembly, Supramolecular Chemistry, Quantum-Size-Related Properties, and Applications Toward Biology, Catalysis, and Nanotechnology. *Chem. Rev.* **2004**, *104*, 293–346.
2. Zhao, W.; Brook, M. A.; Li, Y. Design of Gold Nanoparticle-Based Colorimetric Biosensing Assays. *ChemBioChem* **2008**, *9*, 2363–2371.
3. Baptista, P.; Pereira, E.; Eaton, P.; Doria, G.; Miranda, A.; Gomes, I.; Quaresma, P.; Franco, R. Gold Nanoparticles for the Development of Clinical Diagnosis Methods. *Anal. Bioanal. Chem.* **2008**, *391*, 943–950.
4. Shim, S.-Y.; Lim, D.-K.; Nam, J.-M. Ultrasensitive Optical Biodiagnostic Methods Using Metallic Nanoparticles. *Nanomedicine* **2008**, *3*, 215–232.
5. Gourishankar, A.; Shukla, S.; Ganesh, K. N.; Sastry, M. Isothermal Titration Calorimetry Studies on the Binding of DNA Bases and PNA Base Monomers to Gold Nanoparticles. *J. Am. Chem. Soc.* **2004**, *126*, 13186–13187.
6. Memers, L. M.; Stblom, M.; Zhang, H.; Jang, N. H.; Liedberg, B.; Mirkin, C. A. Thermal Desorption Behavior and Binding Properties of DNA Bases and Nucleosides on Gold. *J. Am. Chem. Soc.* **2002**, *124*, 11248–11249.
7. Jang, N. H. The Coordination Chemistry of DNA Nucleosides on Gold Nanoparticles as a Probe by SERS. *Bull. Korean Chem. Soc.* **2002**, *23*, 1790–1800.
8. Storhoff, J. J.; Elghanian, R.; Mirkin, C. A.; Letsinger, R. L. Sequence-dependent Stability of DNA-Modified Gold Nanoparticles. *Langmuir* **2002**, *18*, 6666–6670.
9. Zhao, W. T.; Thomas, M. H.; Lee, M. H.; Leung, S. S. Y.; Hsing, I.-M. Tunable Stabilization of Gold Nanoparticles in Aqueous Solutions by Mononucleotides. *Langmuir* **2007**, *23*, 7143–7147.
10. Li, H.; Rothberg, L. Colorimetric Detection of DNA Sequences Based on Electrostatic Interactions with Unmodified Gold Nanoparticles. *Proc. Natl. Acad. Sci. U.S.A.* **2004**, *101*, 14036–14039.
11. Li, H.; Rothberg, L. Label-Free Colorimetric Detection of Specific Sequences in Genomic DNA Amplified by the Polymerase Chain Reaction. *J. Am. Chem. Soc.* **2004**, *126*, 10958–1096.
12. Cho, K.; Lee, Y.; Lee, C. H.; Lee, K.; Kim, Y.; Choi, H.; Ryu, P. D.; Lee, S. Y.; Joo, S. W. Selective Aggregation Mechanism of Unmodified Gold Nanoparticles in Detection of Single Nucleotide Polymorphism. *J. Phys. Chem. C* **2008**, *112*, 8629–8633.
13. Rho, S.; Kim, S. J.; Lee, S. C.; Chang, J. H.; Kang, H.; Choi, J. Colorimetric Detection of ssDNA in a Solution. *Curr. Appl. Phys.* **2009**, *9*, 534–537.
14. Gearheart, L. A.; Ploehn, H. J.; Murphy, C. J. Oligonucleotide Adsorption to Gold Nanoparticles: A Surface-Enhanced Raman Spectroscopy Study of Intrinsically Bent DNA. *J. Phys. Chem. B* **2001**, *105*, 12609–12615.
15. Wang, J.; Wang, L.; Li, X.; Liang, Z.; Song, S.; Li, W.; Li, G.; Fan, C. A Gold Nanoparticle-Based Aptamer Target Binding Readout for ATP Assay. *Adv. Mater.* **2007**, *19*, 3943–3946.
16. Wei, H.; Li, B. L.; Wang, E. K.; Dong, S. J. Simple and Sensitive Aptamer-Based Colorimetric Sensing of Protein Using Unmodified Gold Nanoparticle Probes. *Chem. Commun.* **2007**, 3735–3737.
17. Lee, J. H.; Wang, Z. D.; Liu, J. W.; Lu, Y. Highly Sensitive and Selective Colorimetric Sensors for Uranyl (UO_2^{2+}): Development and Comparison of Labeled and Label-Free Dnazyme-Gold Nanoparticle Systems. *J. Am. Chem. Soc.* **2008**, *130*, 14217–14226.
18. Chakrabarti, R.; Klibanov, A. M. Nanocrystals Modified with Peptide Nucleic Acids (PNAs) for Selective Self-Assembly and DNA Detection. *J. Am. Chem. Soc.* **2003**, *125*, 12531–12540.
19. Murphya, D.; Redmonda, G.; Torreb, B. G.; Eritja, R. Hybridization and Melting Behavior of Peptide Nucleic Acid (PNA) Oligonucleotide Chimeras Conjugated to Gold Nanoparticles. *Helv. Chim. Acta* **2004**, *87*, 2727–2734.
20. Kanjanawarut, R.; Su, X. D. Colorimetric Detection of DNA Using Unmodified Metallic Nanoparticles and Peptide Nucleic Acid Probes. *Anal. Chem.* **2009**, *81*, 6122–6129.
21. Zhao, W.; Chiuman, W.; Lam, J. C. F.; Brook, M. A.; Li, Y. Simple and Rapid Colorimetric Enzyme Sensing Assays Using Non-Crosslinking Gold Nanoparticle Aggregation. *Chem. Commun.* **2007**, 3729–3731.
22. Wei, H.; Chen, C.; Han, B.; Wang, E. Enzyme Colorimetric Assay Using Unmodified Silver Nanoparticles. *Anal. Chem.* **2008**, *80*, 7051–7055.

23. Choi, Y.; Ho, N. H.; Tung, C. H. Sensing Phosphatase Activity by Using Gold Nanoparticles. *Angew. Chem., Int. Ed.* **2007**, *46*, 707–709.
24. Oishi, J.; Asami, Y.; Mori, T.; Kang, J. H.; Niidome, T.; Katayama, Y. Colorimetric Enzyme Activity Assay Based on Noncrosslinking Aggregation of Gold Nanoparticles Induced by Adsorption of Substrate Peptides. *Biomacromolecules* **2008**, *9*, 2301–2308.
25. Oishi, J.; Han, X. M.; Kang, J. H.; Asami, Y.; Mori, T.; Niidome, T.; Katayama, Y. High-Throughput Colorimetric Detection of Tyrosine Kinase Inhibitors Based on the Aggregation of Gold Nanoparticles. *Anal. Biochem.* **2008**, *373*, 161–163.
26. Thompson, D. G.; Enright, A.; Faulds, K.; Smith, W. E.; Graham, D. Ultrasensitive DNA Detection Using Oligonucleotide-Silver Nanoparticle Conjugates. *Anal. Chem.* **2008**, *80*, 2805–2810.
27. Lee, J. S.; Lytton-Jean, A. K. R.; Hurst, S. J.; Mirkin, C. A. Silver Nanoparticle-Oligonucleotide Conjugates Based on DNA with Triple Cyclic Disulfide Moieties. *Nano Lett.* **2007**, *7*, 2112–2115.
28. Lao, A. I. K.; Su, X. D.; Khin, M. M. A. SPR Spectroscopy Study DNA Hybridization with DNA and PNA Probes under Stringent Conditions. *Biosens. Bioelectron.* **2009**, *24*, 1717–1722.
29. Grabar, K. C.; Freeman, R. G.; Hommer, M. B.; Natan, M. J. Preparation and Characterization of Au Colloid Monolayers. *Anal. Chem.* **1995**, *67*, 735–743.
30. Jin, R.; Wu, G.; Li, Z.; Mirkin, C. A.; Schatz, G. C. What Controls the Melting Properties of DNA-Linked Gold Nanoparticle Assemblies. *J. Am. Chem. Soc.* **2003**, *125*, 1643–1654.
31. Yguerabide, J.; Yguerabide, E. E. Light-Scattering Submicroscopic Particles as Highly Fluorescent Analogs and Their Use as Tracer Labels in Clinical and Biological Applications. I. Theory. *Anal. Biochem.* **1998**, *262*, 137–156.
32. Yguerabide, J.; Yguerabide, E. E. Light-Scattering Submicroscopic Particles as Highly Fluorescent Analogs and Their Use as Tracer Labels in Clinical and Biological Applications. II. Experimental Characterization. *Anal. Biochem.* **1998**, *262*, 157–176.